Atmos. Chem. Phys. Discuss., 10, 13055–13090, 2010
www.atmos-chem-phys-discuss.net/10/13055/2010/
doi:10.5194/acpd-10-13055-2010

Atmospheric Chemistry and Physics Discussions

CO_2, $\delta O_2/N_2$ and APO: observations from the Lutjewad, Mace Head and F3 platform flask sampling network

I. T. van der Laan-Luijkx[1,], U. Karstens[2], J. Steinbach[2], C. Gerbig[2], C. Sirignano[1,*], R. E. M. Neubert[1], S. van der Laan[1,**], and H. A. J. Meijer[1]**

[1]Centre for Isotope Research (CIO), University of Groningen, Groningen, The Netherlands
[2]Max Planck Institute for Biogeochemistry, Jena, Germany
[*]currently at: CIRCE, Department of Environmental Sciences, Second University of Napels, Caserta, Italy
[**]currently at: Climate and Environmental Physics, Physics Institute, University of Bern, Bern, Switzerland

Received: 5 March 2010 – Accepted: 14 April 2010 – Published: 21 May 2010

Correspondence to: I. T. van der Laan-Luijkx (i.t.luijkx@rug.nl)

Published by Copernicus Publications on behalf of the European Geosciences Union.

Abstract

We report results from our atmospheric flask sampling network for three European sites: Lutjewad in the Netherlands, Mace Head in Ireland and the North Sea F3 platform. The air samples from these stations are primarily being analyzed for their CO_2 and O_2 concentrations. In this paper we present the CO_2 and O_2 data series from these sites between 1998 and 2009, as well as the atmospheric potential oxygen (APO). The seasonal pattern and long term trends agree to a large extent between our three measurement locations. We however find an increasing gradient between Mace Head and Lutjewad, both for CO_2 and O_2. As Lutjewad is influenced by local fluctuations in the fossil fuel sources, we use an atmospheric transport model in combination with CO_2 emission data and information on the fossil fuel mix per region and category in order to correct the tracer APO for a residual fossil fuel component. For Lutjewad this correction differs significantly from the global average. Using the APO trend from Mace Head we obtain an estimate for the global oceanic CO_2 uptake of 1.8 ± 0.8 PgC/year.

1 Introduction

Climate change and its causes and effects have been a subject of intensive research during the past decades. Climate change is primarily induced by changes in the atmosphere's composition, specifically the rapid increase in the concentrations of the greenhouse gases CO_2, CH_4, N_2O and halocarbons (e.g. IPCC, 2007). Anthropogenic carbon dioxide is the most significant contributor to climate change, therefore a thorough comprehension of the global carbon cycle and the main processes involving CO_2 is essential.

Combined atmospheric O_2 and CO_2 measurements yield valuable information about carbon cycle processes, that cannot be acquired from measurements of CO_2 concentrations alone (e.g. Bender et al., 1996; Keeling and Garcia, 2002; Keeling et al., 1993; Keeling and Shertz, 1992; Manning and Keeling, 2006). Most processes show an

ACPD
10, 13055–13090, 2010

inverse relationship between O_2 and CO_2 (e.g. fossil fuel combustion, photosynthesis and respiration), but in the exchange between the ocean and the atmosphere O_2 and CO_2 are uncoupled. Marine CO_2 uptake leads to a chemical reaction with the ocean water, leading to a CO_2 buffer effect. The uptake of O_2 does not have this effect, as O_2 merely dissolves in water and this is independent of the CO_2 uptake process. Combined measurements of atmospheric O_2 and CO_2 can therefore be used to partition land and ocean CO_2 uptake (e.g. Battle et al., 2000; Bender et al., 2005; Keeling and Shertz, 1992; Langenfelds et al., 1999; Manning and Keeling, 2006).

Since changes in the atmospheric O_2 concentration are in most processes directly related to changes in the CO_2 concentrations, they occur in the same order of magnitude. However, the changes in O_2 are harder to detect as they are to be measured against a much larger background. High precision measurements of atmospheric O_2 have begun in 1988 when R. F. Keeling developed an instrument based on interferometry (Keeling, 1988a, b). Since then other methods have been developed to enable atmospheric O_2 measurements at the required precision of $1{:}10^6$ (WMO, 2009). Current techniques include mass-spectrometry (Bender et al., 1994), paramagnetic analyzers (Manning et al., 1999), vacuum ultraviolet absorption (Stephens, 1999; Stephens et al., 2003), gas chromatography (Tohjima, 2000) and fuel cells (Patecki and Manning, 2007; Stephens et al., 2007; Thompson et al., 2007). Each of these techniques has its specific advantages and disadvantages, not only related to the O_2 sensor obtaining the required precision, but also to the possibility to run the instrument automatically, remotely or in harsh conditions, e.g. on moving platforms, like ships or aircrafts.

The first systematic measurements of atmospheric O_2 were performed by Keeling and Shertz (1992) at three measurement sites from north to south: Alert (82.5° N, 62.3° W), La Jolla (32.9° N, 117.3° W) and Cape Grim (40.7° S, 114.7° E), showing seasonal patterns and interannual O_2 variations in different environments on both hemispheres. Since then the amount of sampling sites has increased during the past two decades from these three to over 20, including both stations where air flasks are sampled as well as those with continuous monitoring of atmospheric O_2 (e.g. Battle et al.,

ACPD
10, 13055–13090, 2010

2006; Kozlova et al., 2008; Manning and Keeling, 2006; Popa et al., 2009; Thompson et al., 2009; Tohjima et al., 2008). In this paper we will contribute new observations from the flask sampling stations Lutjewad in the Netherlands, Mace Head in Ireland and the F3 North Sea platform, extending earlier work presented by Sirignano et al. (2010). For the F3 North Sea platform we also combine the flask samples with the first continuous onsite measurements (van der Laan-Luijkx et al., 2010).

In this paper we first describe the measurement stations (Sect. 2), and continue with the flask sampling strategies and measurement methods (Sect. 3.1). Sections 3.2 and 3.3 give background information on the O_2 calculations and Atmospheric Potential Oxygen (APO). The regional model REMO, which we use to correct APO for the fossil fuel influence is described in Sect. 3.4. since for our coastal station Lutjewad the fossil fuel influences on APO are not negligible. In the Sect. 4 we present our observations of CO_2, O_2 and APO at the three stations and discuss their variability, trends and gradients. Finally, we estimate the adjusted fossil fuel oxidative ratios and give an estimate for global marine CO_2 uptake.

2 Descriptions of the measurement stations

Figure 1 shows the locations of our three monitoring stations. The Lutjewad atmospheric monitoring station is situated on the northern coast of the Netherlands, at 53°24′ N, 6°21′ E, 1 m a.s.l, alongside the Wadden Sea. The station comprises a 60 m high tower as well as a laboratory with an automated flask sampler and instruments for in-situ measurements. Several atmospheric gases and other characteristics are measured at Lutjewad including continuous measurements of CO_2, CH_4, CO, N_2O, SF_6, ^{222}Rn and biweekly integrated sampling of $\Delta^{14}C$, as presented by van der Laan et al. (2009a, b). Basic meteorological conditions are monitored at all sites, including wind speed and direction, temperature, atmospheric pressure and relative humidity. The main wind direction is between southwest and west (van der Laan et al., 2009c), which implies a continental contribution with the main wind direction.

ACPD
10, 13055–13090, 2010

Mace Head atmospheric research station (53°20′ N, 9°54′ W) is located on the west coast of Ireland. With the prevalent wind direction from the western section, the station is ideal for sampling background air masses originating from the Atlantic Ocean. Further details on Mace Head atmospheric research station are provided by e.g. Derwent et al. (2002) and Jennings et al. (1993). At Mace Head air samples were collected form 35 m a.s.l. during restricted baseline conditions (Bousquet et al., 1996).

The sea based measurement station F3 is situated on a North Sea oil and gas platform (54°51′ N, 4°44′ E), around 200 km north of the Dutch coast. The platform produces oil and gas and is operated by Gaz de France (GdF Suez). Like Lutjewad atmospheric monitoring station, the F3 station contains an automated flask sampler, as well as a set-up for continuous monitoring of atmospheric CO_2 and O_2 concentrations (van der Laan-Luijkx et al., 2010). The continuous measurements of O_2 are performed with an Oxzilla II instrument (fuel cells) and CO_2 is measured using infrared absorption (CarboCaps, Vaisala). The air inlets of both the flask autosampler and the continuous measurement setup are situated on the top deck at 46 m a.s.l. The depth of the North Sea at this location is 44 m and the prevalent wind direction at F3 is southwest. Flasks are filled when the wind direction is between south and west. We thereby sample mainly the coastal marine section of the north-western part of the European continent.

3 Methods

3.1 Flask sampling and measurement techniques

Since the end of 2000 weekly air samples are taken at Lutjewad from the air inlet at the top of the tower (60 m) using a remotely controlled flask sampler (Neubert et al., 2004). This sampler fills 2.5 l flasks with dried air at a specified time interval and accommodates the possibility to fill up to 20 flasks. The sampler consists of a manifold with valves to select the individual flasks for filling and a cryocooler for air drying. The automated air drying system is described by Neubert et al. (2004) with additional

ACPD
10, 13055–13090, 2010

information given by van der Laan-Luijkx et al. (2010). Each flask is flushed with dried air for 60 min before the automated system closes the flask and continues to the next flask. At F3 the same system is used, but due to space limitations a maximum of 10 flasks is connected to the system at a time. The glass flasks used have glass valves from Louwers (Hapert, the Netherlands) with viton o-rings and Rotulex connections. The valves are operated using electric valve actuators designed at the Centre for Isotope Research (CIO, Groningen, the Netherlands). At Mace Head, identical flasks are manually filled in pairs every two weeks.

The flasks are analyzed in the CIO laboratory for their concentrations[1] of CO_2, CH_4 and CO, as well as for $\delta O_2/N_2$, $\delta^{13}CO_2$, $\delta CO^{18}O$ and $\Delta^{14}CO_2$. $\delta O_2/N_2$ is measured using a Micromass Optima dual inlet isotope ratio mass spectrometer (DI-IRMS), in a similar manner as Bender et al. (1994). The concentrations of CO_2, CH_4 and CO are measured using a Hewlett-Packard gas chromatograph (GC), model 6890, comparable to the setup described by Worthy et al. (2003). More details on the measurement instruments are presented by Sirignano et al. (2010).

3.2 O_2/N_2 calculations and calibration

Changes in the atmospheric O_2 concentration are usually reported as the changes in the ratio of O_2 to N_2. As the atmospheric N_2 concentration is much less variable, the changes in the O_2/N_2 ratio mainly represent changes in the O_2 concentration. Unlike the O_2 concentration, the O_2/N_2 ratio is insensitive to the changes in other atmospheric gases, such as CO_2. Changes in the O_2/N_2 ratio of a sample are expressed as relative deviations from a known reference gas, as shown in Eq. (1) (Keeling and Shertz, 1992).

$$\delta(O_2/N_2) = \frac{(O_2/N_2)_{sample}}{(O_2/N_2)_{reference}} - 1 \quad (1)$$

[1] In this paper the more correct term mixing ratio has been substituted by concentration to avoid confusion with the term O_2/N_2 ratio.

ACPD
10, 13055–13090, 2010

For natural air, the $\delta O_2/N_2$ values are relatively small and are therefore multiplied with 10^6 and expressed in per meg. While mass spectrometers measure $\delta O_2/N_2$ directly, other methods measure the O_2 concentration. To correct for changes in the O_2 concentration caused by changes in the CO_2 concentration, simultaneous measurements of CO_2 are required for these methods. Equation (2) (Kozlova et al., 2008; Stephens et al., 2003) shows the relationship between changes in the O_2 concentration and changes in $\delta O_2/N_2$.

$$\delta(O_2/N_2) = \frac{\delta XO_2 + (\Delta CO_2 \cdot S_{O_2})}{(1 - S_{O_2}) \cdot S_{O_2}} \text{ (in per meg)} \quad (2)$$

Here, S_{O_2} = 0.20946 (Machta and Hughes, 1970) represents the standard mole fraction of oxygen in air and δXO_2, ΔCO_2 and $\delta O_2/N_2$ are the changes in the O_2 mole fraction, the CO_2 concentration and the O_2/N_2 ratio respectively. A change of 1 ppm in the O_2 mole fraction without any concurrent change in CO_2 therefore causes a change of 6.04 per meg in $\delta O_2/N_2$, while an exchange of a certain amount of O_2 molecules for the same amount of CO_2 molecules causes a change of 4.77 per meg in $\delta O_2/N_2$.

Earlier work by Sirignano et al. (2010) showed the atmospheric oxygen concentrations from Lutjewad and Mace Head presented on the internally used CIO scale, stating the need for an adaptation to an internationally used scale for intercomparison of the measurement accuracy as well as data comparison. The complete data series was recalibrated using three cylinders spanning from −805 to −258 per meg provided by the Scripps Institution of Oceanography (SIO). The mass spectrometer measures each sample twice against a machine reference gas (i.e. the reference in Eq. (1). Besides the samples, working gas cylinders were measured following an identical procedure as for the samples. Each measurement gives the difference between the sample or working gas and the machine reference gas. The calibration procedure included a drift correction of this difference based on the measurements of a suite of working cylinders against the machine reference gas. The amount of working gas cylinders used has increased over time from one cylinder to four, which makes the latest data more

ACPD
10, 13055–13090, 2010

accurate than the earlier data. During the start-up phase of the measurements, the machine reference gas has been changed several times, requiring a scale conversion for each change. The SIO primary cylinders were measured only against the current machine reference gas, which makes the data of samples measured (i.e. not necessarily sampled) after 2006 the most accurate.

For the CO_2 concentration, each flask is measured at least two times on our GC in order to enhance the measurement precision. A working standard is measured after every second sample measurement, and the measurement sequence included a target cylinder for quality control. The GC measurements are calibrated on a regular basis with a suite of standards provided by the World Meteorological Organization (WMO). The final CO_2 concentration of the flask samples is expressed in ppm on the WMO X2007 scale.

3.3 Atmospheric Potential Oxygen (APO) and APO*

Stephens et al. (1998) have defined the tracer Atmospheric Potential Oxygen (APO), as shown in Eq. (3).

$$\delta\mathrm{APO} = \delta\mathrm{O_2/N_2} + \frac{1.1\cdot(\mathrm{CO_2} - 350)}{S_{\mathrm{O_2}}} (\text{ per meg}) \quad (3)$$

APO is the sum of $\delta O_2/N_2$ plus 1.1 times the CO_2 concentration, with 1.1 being the global average stoichiometric ratio (α_B) between O_2 and CO_2 in photo-synthesis and respiration processes (Severinghaus, 1995). S_{O_2} is the standard mole fraction of oxygen in air. An arbitrary reference of 350 ppm is subtracted from the CO_2 concentration, as used on the SIO per meg scale for APO (Manning and Keeling, 2006). The definition implies that APO is unaffected by activity of land biota and is therefore sensitive principally to ocean-atmosphere exchange of O_2 and CO_2, but also still partly to fossil fuel combustion and its specific oxidation ratio (OR = O_2:CO_2). The global average OR for fossil fuel is α_F = 1.4 (Keeling, 1988b). Therefore the APO on average still includes 0.3 times the fossil fuel combustion contribution, which can be seen from the global

ACPD
10, 13055–13090, 2010

budgets for CO_2, O_2 and APO (in moles) in Eq. (4) through (6) (Manning and Keeling, 2006).

$$\Delta CO_2 = F - B - O \quad (4)$$

$$\Delta O_2 = -\alpha_F F + \alpha_B B + Z \quad (5)$$

$$\Delta APO = \Delta O_2 + \alpha_B \Delta CO_2 = (\alpha_B - \alpha_F) F - \alpha_B O + Z \quad (6)$$

Where ΔCO_2 and ΔO_2 are the changes in the atmospheric concentration of CO_2 and O_2 respectively, expressed in moles. F is the CO_2 emission to the atmosphere originating from fossil fuel combustion and cement manufacture. B is the net terrestrial biosphere uptake of CO_2 from the atmosphere. O is marine CO_2 uptake and Z is the net marine O_2 exchange. As both the CO_2 fossil fuel source and the CO_2 biosphere sink are directly coupled to the changes in the O_2 concentration, they are included in the relationship for O_2 with their respective molar exchange ratios (α_B and α_F respectively). The marine processes involving CO_2 and O_2 are not coupled, and they are therefore represented by different symbols (O and Z). The relationship for APO as represented in (Eq. 6) shows that APO is unaffected by biosphere activity.

As APO is defined to estimate marine CO_2 uptake, the remaining influence of fossil fuel combustion should be accounted for. Sirignano et al. (2010) therefore suggest the use of a modified version of APO, named APO*, which is defined in Eq. (7) and is truly only sensitive to ocean-atmosphere exchange.

$$\Delta APO^* = \Delta APO - (\alpha_B - \alpha_F) F \quad (7)$$

The oxidative ratio for fossil fuel combustion (α_F) varies over the globe, depending on the types of fossil fuels that are used in each country. The oxidative ratios for the individual fossil fuel types are: 1.17 for coal, 1.44 for oil and 1.95 for natural gas (Keeling, 1988a). Biofuels have the lowest OR, around 1.1, which is identical to the ratio for biospheric release. Therefore combustion of biofuels is also removed from the APO signal like the terrestrial biosphere. In the Netherlands the fossil fuel OR is

ACPD
10, 13055–13090, 2010

higher than average (around 1.7), because of the high share of natural gas which also significantly varies within the different seasons. In order to correct for this deviation from the average OR for fossil fuel a modelling study was performed to estimate the regional OR for our three measurement locations, which is described in the following section.

3.4 REMO

The REgional MOdel (REMO) (Chevillard et al., 2002; Langmann, 2000) is an atmospheric transport model covering the European continent. The model's grid resolution is $0.5^{\circ} \times 0.5^{\circ}$ in a rotated spherical coordinate system, corresponding to a grid cell resolution of approximately 55×55 km. The atmosphere is divided in 20 vertical levels, of which we use the lowest level between 0 and 65 m, corresponding to the height of our sampling sites. The initial and lateral boundary conditions for the meteorology were based on the ECMWF (European Centre for Medium-Range Weather Forecasts) analysis and for CO_2 and APO the TM3 global transport model was used. The surface fluxes for the oceanic APO were calculated from TM3 inversion of atmospheric CO_2 and O_2 concentrations (Rödenbeck et al., 2008). For the fossil fuel part, hourly fluxes of CO_2 emissions and O_2 uptake from the CO_2 release and Oxygen uptake from Fossil Fuel Emissions Estimate (COFFEE) dataset (Steinbach et al., 2010) were used as input for the model. This dataset combines CO_2 emissions from the Emission Database for Global Atmospheric Research (EDGAR) inventory version 3.2 (Olivier and Berdowski, 2001) extrapolated to 2006 using BP fossil fuel consumption data at national level (available at http://www.bp.com/statisticalreview) with fossil fuel type specific oxidative ratios derived from fuel consumption data from the UN energy statistics (http://www.data.un.org). Seasonal and diurnal variations of the emissions were included based on time profiles available in the EDGAR database. Figure 2a shows the global distribution of the oxidative ratios from fossil fuel combustion for 2006 and Fig. 2b shows the region of our sampling locations in more detail (Steinbach et al., 2010). The oxidative ratios obtained from these datasets for the fossil fuel emissions

ACPD
10, 13055–13090, 2010

at the locations of our sites, averaged over 2006, are: 1.64 for Lutjewad, 1.49 for Mace Head and 1.44 for F3. As Lutjewad is located in a grid cell with no data available in the EDGAR database, we have used the data from the closest grid cell. The obtained oxidative ratios are based on the information from the described datasets, and are not necessarily the same as the observed oxidative ratios, which are subjected to atmospheric transport and mixing.

4 Results

4.1 CO_2 and O_2

Air flasks have been filled at Lutjewad since October 2000, at Mace Head since December 1998 and at the F3 North Sea platform since June 2006. The data series for the atmospheric concentrations of O_2 and CO_2 from flask samples between 2000 and 2005 from Lutjewad and Mace Head have been presented by Sirignano et al. (2010). In this section we present the follow-up of this work with extended data series until 2009. In addition, for F3 half-hourly averaged continuous measurements are available from September 2008 to June 2009 as described by van der Laan-Luijkx et al. (2010). The continuous O_2 record presented in that paper has also been converted to the internationally used Scripps scale – as the flask data – to be able to make a direct comparison.

Flasks which were suspected to have been contaminated, e.g. by leaks in the sampling or measurement system or due to long storage of the flasks (Sturm et al., 2004) have been removed from the data set, as well as those flasks which were marked as locally influenced samples or samples with a continental trajectory. At Lutjewad these samples were identified using the concentration of ^{222}Rn, which has been measured simultaneously at Lutjewad since 2005. ^{222}Rn is a radioactive noble gas emanating from soils. The emissions of ^{222}Rn from oceans is very small, therefore these characteristics can be used to determine whether the air masses have been influenced by continental emissions. Therefore, all flasks with a ^{222}Rn concentration higher than 3 Bq/m^3 are disregarded as they represent air with continental influences and are not

ACPD
10, 13055–13090, 2010

background air. As we did not measure ^{222}Rn before 2005 at Lutjewad and not at all at Mace Head and F3, the ^{222}Rn concentrations have been correlated with the CO concentrations at Lutjewad, leading to an exclusion of the flask samples containing CO concentration higher than 200 ppb. We subsequently used this criterion for the exclusion of flask samples at Mace Head and F3. For Mace Head only a small amount of flasks were excluded as they were sampled during restricted base line conditions.

For both O_2 and CO_2 the data have been filtered, based on a fit through the data points. The used fit is a linear combination of a three harmonic seasonal component and a linear trend. Data points with residuals larger than 2.5 times the standard deviation from the original fit have been excluded. For F3 we have used the data from both the flasks and the continuous measurements to improve the quality of the fit (compared to fitting flask data only). Our fitting strategy is slightly different from that used in Sirignano et al. (2010) in that we have chosen a linear trend fit instead of a Loess trend fit. The Loess trend fit is very sensitive to unevenly time-distributed data. As our data series have several gaps and more (not-excluded) flask samples in certain periods, the Loess fit does not provide valid information on the trend variability.

Figure 3 shows the observations from each station for CO_2 and O_2 respectively. The expected seasonal patterns are clear in the data series of all three sites as well as the long term trends, slowly increasing for CO_2 and a concurrent decreasing trend for O_2. An overview of the obtained fit parameters is presented in Table 1. A comparison of the obtained fit results of our three measurement locations is shown in Fig. 4. The three harmonic fits of the detrended seasonal cycles for both CO_2 and $\delta O_2/N_2$ are shown in Fig. 5.

For Lutjewad we find a seasonal (peak-trough) amplitude of 12.0 ± 0.6 ppm for CO_2 and 114 ± 8 per meg for $\delta O_2/N_2$. For Mace Head we find a seasonal amplitude of 14.0 ± 0.3 for CO_2 and 142 ± 6 per meg for $\delta O_2/N_2$. When comparing the seasonality from both locations to previous studies, we see some differences. Firstly, the seasonal amplitude of Lutjewad is lower in our case than the 16.1 ± 0.4 ppm presented by Sirignano et al. (2010) and the 14 ppm from the continuous observations from van der

ACPD
10, 13055–13090, 2010

Laan et al. (2009b). However, the seasonal amplitude of Mace Head is the same as in Sirignano et al. (2010). The fact that our obtained amplitude for Lutjewad is lower than in both other studies is likely to be caused by inadequate representation of the seasonal cycle in the fit. As can be seen from Fig. 3a, several data points in the troughs are lower than the fit and are therefore probably not well reflected in the fit, due to a too low sampling frequency in the narrow trough periods. For F3 we find a seasonal amplitude of 15.2 ± 0.1 ppm for CO_2 and 144 ± 2 per meg for $\delta O_2/N_2$. Even though the record at F3 is still short, the quality of the seasonal component in the fit is considerably higher here, thanks to the continuous data. Figure 5 shows more clearly than Fig. 3 that the start of the growing season at Lutjewad (and also at F3) begins earlier than at Mace Head, showing that the influence of the land biota is more visible in the Lutjewad signal.

The seasonal amplitudes for CO_2 and $\delta O_2/N_2$ from other stations within Europe are presented in Table 2. Their locations are included in Fig. 1 using abbreviated station names. It can be seen that the highest seasonal amplitudes for CO_2 are found at the eastern continental sites Bialystok and ZOTTO. The seasonal cycles from Mace Head, F3 and Lutjewad (when taking into account that the estimate of 12.0 is likely to be too low) compare best to observations from Ochsenkopf and the Shetland Islands. The Ochsenkopf amplitudes are given from the highest level in the tower (163 m) which is generally above the boundary layer, which decreases local influences. Jungfraujoch has a much lower CO_2 seasonal amplitude due to its high altitude of 3580 m above sea level which causes it to be far above the planetary boundary layer and thereby sampling European background air masses. The amplitudes of the seasonal cycles of $\delta O_2/N_2$ from our three sites vary more than for CO_2. Again, the seasonal amplitude of Lutjewad is probably underestimated; therefore Lutjewad compares best to Ochsenkopf and ZOTTO regarding their seasonal amplitudes. The seasonal amplitudes at Mace Head and F3 are slightly higher, 142 and 144 per meg, with both stations sampling only the marine sectors. The seasonal amplitude at Jungfraujoch is again much lower due to the sampled background air masses.

ACPD
10, 13055–13090, 2010

4.2 Trend analysis

The long term trend in the Lutjewad CO_2 concentration from Fig. 3a is estimated at 1.97 ± 0.07 ppm/year for CO_2 and -21.0 ± 0.9 per meg/year for $\delta O_2/N_2$. At Mace Head the long term trend is found to be 1.90 ± 0.04 ppm/year for CO_2 and -18.5 ± 0.7 per meg/year for $\delta O_2/N_2$. Since the data series at the F3 platform is only 3 years the long term trends cannot provide as accurate information on the trends, which are estimated at 2.11 ± 0.04 ppm/year for CO_2 and -27.1 ± 0.6 per meg/year for $\delta O_2/N_2$ (the errors given are the fit errors and do not necessarily reflect the total error including systematic and measurement errors). Thanks to the longer sampling period, our trend estimates are now much more accurate than those presented by Sirignano et al. (2010), but the results correspond well to each other within the uncertainty range. The long-term trends for CO_2 and $\delta O_2/N_2$ for other European sites are included in Table 2. The CO_2 trends at all sites are close to each other at about 2 ppm/year. The trends for $\delta O_2/N_2$ are all close to -20 per meg/year, except for Jungfraujoch.

Figure 4a shows a comparison of the fits of CO_2 from our three measurement locations to the marine background layer reference from the GLOBALVIEW-CO_2 (2008) database for the same latitude (53° N). From this figure we can conclude that the fits of the Lutjewad, Mace Head and F3 data correspond well to the GLOBALVIEW-CO_2 signal when comparing the timing of the growing season. The sharp decrease marking the uptake of CO_2 by the land biota and the slower increase at the end of the growing season are clearly reflected in all fits and compare well to that of GLOBALVIEW-CO_2. The CO_2 signal from Lutjewad follows the GLOBALVIEW-CO_2 signal well, except for the depth of the troughs in the growing season. When looking at the data points in Fig. 3a, we can see that several measurements indicate a lower summer CO_2 value for Lutjewad, which is not reflected in the fit. As Lutjewad is influenced by continental air masses with southern and eastern winds, the signal is frequently influenced by local (or continental) anthropogenic sources, concealing the biosphere signal. Due to the short period with the lowest yearly CO_2 values, a higher sampling frequency is

ACPD
10, 13055–13090, 2010

recommendable for this period during summer. The seasonal amplitude at Lutjewad as estimated from the fit is therefore likely to be higher than that presented in Table 1. As mentioned before, the start of the growing season at Lutjewad is slightly earlier than the background reference, which is related to the continental influence at Lutjewad, sampling the land biota directly close to the source. For the short overlapping period of the data from the F3 platform and the GLOBALVIEW-CO_2 background reference the F3 signal is in good agreement with the GLOBALVIEW-CO_2 signal, however the signal at F3 is slightly higher. Figure 4b shows the same comparison between the fit results of the data from the three locations for $\delta O_2/N_2$ (a $\delta O_2/N_2$ GLOBALVIEW background reference is currently not available).

The most striking feature from Fig. 4a is the offset between the Mace Head signal and the signal from Lutjewad. The Mace Head signal is also showing a significant negative offset from the marine background signal GLOBALVIEW-CO_2 especially during winter. This gradient increases slightly over time. This is in agreement with the observations from Ramonet et al. (2010). They found that the difference between the CO_2 concentration at Mace Head and fourteen other measurement stations in continental Europe was increasing during the time period 1995–2007. Their obtained mean ΔCO_2 (i.e. $[CO_2]_{\text{measurement site}} - [CO_2]_{\text{Mace Head}}$) for all stations increased by 1–2 ppm during 1990–1995 and 2000–2005. Our increase in the CO_2 gradient over the measurement period 2001–2008 between Lutjewad and Mace Head (ΔCO_2 = 0.5 ppm) fits well into the general picture presented by Ramonet et al. (2010). New is the $\delta O_2/N_2$ gradient and its gradual increase that we present in Fig. 4b. For $\delta O_2/N_2$ we observe that the gradient is also increasing (negatively). We find a change in the gradient between Lutjewad and Mace Head of −20 per meg over the total period 2001–2008. Ramonet et al. (2010) attributed the increasing gradient in CO_2 to a combination of a shallower boundary layer height and regional changes in emissions. Based on the CO_2 gradient of 0.5 ppm, we would expect an increasing (negative) gradient for $\delta O_2/N_2$ of −3.4 per meg. The large difference between our observed increasing gradient and the expected increase in the gradient based on a higher fossil fuel consumption implies another

ACPD
10, 13055–13090, 2010

major contribution to the increasing $\delta O_2/N_2$ gradient. One possible contributing factor could be an increasing share of natural gas in the fossil fuel mix in the continent. This increase could be observed at Lutjewad, but not at Mace Head, due to the sampling protocol limited to restricted baseline conditions. However, no shift in the fossil fuel mix is observed in the BP consumption statistics. The continuous difference in the oxidative ratio between the Netherlands and Mace Head creates an O_2 gradient, however whether this gradient can continue to exist and even increase greatly does imply that the gradient is not reduced by transport of O_2 from adjacent regions.

Alternatively, the increasing CO_2 gradient between Mace Head and Lutjewad could in principle also originate from a decreasing atmospheric CO_2 trend at Mace Head due to an increased CO_2 uptake by the North Atlantic. Oceanographic research has shown that the North Atlantic CO_2 sink has varied substantially over the past years, and has also decreased during certain periods (e.g. Corbière et al., 2007; Schuster and Watson, 2007; Watson et al., 2009). Our observed steeper increase in the $\delta O_2/N_2$ gradient compared to CO_2 does not leave much room for an increasing North Atlantic CO_2 uptake during 2000–2008 as marine CO_2 uptake is not coupled to O_2, therefore an increasing North Atlantic CO_2 sink would not explain both gradients simultaneously.

Ramonet et al. (2010) found a higher gradient in winter, which supports the suggestion of a higher natural gas share in the fossil fuel mix, as gas consumption is relatively (and absolutely) higher in winter than in summer. A difference in the seasonal variations in the gradients between Lutjewad and Mace Head for CO_2 and $\delta O_2/N_2$ cannot be derived from the obtained seasonal variations (as shown in Fig. 5). Considering the large amount of scatter in the Lutjewad measurements in Fig. 3, the summer-winter differences in the gradient between Lutjewad and Mace Head cannot be estimated accurately from our records.

ACPD
10, 13055–13090, 2010

4.3 APO

For each measurement site, atmospheric potential oxygen (APO) has been calculated using the observed CO_2 and O_2 concentrations and Eq. (3). The results for APO are shown in Fig. 6 for Lutjewad (a), Mace Head (b) and F3 (c) and are fitted with a linear combination of a three harmonic function and a linear trend, like for CO_2 and $\delta O_2/N_2$ (the fit parameters are shown in Table 1). The seasonal amplitudes of APO are roughly half of that of $\delta O_2/N_2$, as expected. The amplitudes for our three measurement sites are: 64 ± 6 per meg for Lutjewad, 74 ± 6 per meg for Mace Head and 111 ± 2 per meg for F3. The annual long term trend for each site is: -10.6 ± 0.7 per meg/year for Lutjewad and -8.4 ± 0.7 per meg/year for Mace Head. The data series for F3 is not long enough yet to provide precise information on the trend, which is roughly estimated at -13.2 ± 0.5 per meg/year (again, the errors given are the fit errors and are higher when considering the total error). The APO fit can also be calculated using the respective CO_2 and $\delta O_2/N_2$ fits, this does not yield significantly different results. Consistently with the obtained increasing gradients between Lutjewad and Mace Head, the gradient in APO is also increasing between both sites. As the terrestrial biosphere is removed from the APO signal and the fact that the gradient in O_2 is still present in APO, this implies a relation with either the ocean or fossil fuel combustion.

For comparison, the seasonal amplitudes and annual trends for APO from other European stations are shown in Table 2. The seasonal amplitudes at our sampling sites are higher than those from most other continental European stations. As APO primarily reflects the oceanic signal, the difference between the continental sites and the coastal marine sites is expected. The APO signal at the Shetland Islands also shows a higher amplitude. The long-term trends are not available for all sites, mainly because of the short time series.

ACPD
10, 13055–13090, 2010

4.4 Seasonal oxidative ratios

REMO simulations were performed for the year 2006, using the CO_2 emission data and the fuel mix specific oxidative ratios for the fossil fuel related O_2 sink, as described in Sect. 3.4. Since REMO is a regional model, the OR can be calculated directly as the ratio of the resulting atmospheric O_2 and CO_2 concentrations within the model's domain. For 2006 this yielded a seasonal signal for the observed fossil fuel OR (as simulated by REMO) for each of our three measurement locations as shown in Fig. 7. The OR at our three locations is structurally higher than the global average fossil fuel OR of 1.4. The deviation is more pronounced in the simulations for Lutjewad and F3 than for Mace Head. As expected the OR of the fossil fuel emissions in the Netherlands is highly influenced by the high natural gas share in the fossil fuel mix, as was shown in Fig. 2. As the CO_2 emissions and APO are transported by the model, the mixing with emissions from surrounding countries decreases the OR of the observed fossil fuel CO_2 at Lutjewad in comparison to the actual local emissions. The same mixing occurs at the other two sites and is obvious for F3, as the local emissions in the F3 area (according to the EDGAR database) are only influenced by international shipping, the mixing with the emissions from e.g. the Netherlands increases the OR signal. Furthermore, the OR of all three sites clearly shows a seasonal pattern, which has its maximum in winter, when the share of natural gas in the fossil fuel use is higher as it is the main source for (domestic) heating purposes.

4.5 Estimating global marine CO_2 uptake

We estimate the global marine CO_2 uptake using the definitions presented in Manning and Keeling (2006). The net global oceanic CO_2 uptake is calculated as shown in Eq. (8).

$$O = \left[(-\Delta(\delta\mathrm{APO})\cdot 10^{-6}\cdot S_{O_2}\cdot M_{air}\cdot M_C) + (\alpha_B - \alpha_F)F + \left(\frac{Z_{eff}}{M_C}\right)\right]\cdot\frac{1}{\alpha_B} \quad (8)$$

ACPD
10, 13055–13090, 2010

Where $\Delta(\delta APO)$ is the observed annual change in δAPO (in per meg), S_{O_2} = 0.20946 is the standard mole fraction of oxygen (Machta and Hughes, 1970), $M_{air} = 1.769 \times 10^{20}$ mol is the number of moles of dry air in the total atmosphere and M_C = 12.01 g/mol is the molar mass of carbon. The net oceanic outgassing of O_2 is represented as Z_{eff}. We use Z_{eff} = 0.48 PgC/year from Manning and Keeling (2006). The global average molar stoichiometric ratios α_B and α_F are 1.1 and 1.4 respectively. For the fossil fuel emissions F we use the average annual emission, which is 7.7 PgC/year during the period 2000–2009 and 7.5 PgC/year during 1998–2009 (Boden et al., 2009).

The trend in APO at Lutjewad from the flask measurements is -10.6 ± 0.7 per meg/year during the period 2000–2008. As shown in Fig. 7, the oxidative ratio for fossil fuel combustion as perceived at Lutjewad is higher than the global average. Therefore we can correct the oceanic uptake of CO_2 using Eq. (8) as calculated from the APO trend at Lutjewad by using the perceived α_F. To estimate the corrected α_F we have used the average of the minimum daily OR as calculated by REMO, since this is closest to the conditions of the flask samples included in the record, as the flasks are sampled and filtered to represent the background conditions. This leads to an OR of 1.46. Using this corrected α_F value, we estimate the global oceanic uptake O, using Eq. (8), based on the annual change in APO at 2.2 ± 0.8 PgC/year. The correction of the estimation of the global oceanic CO_2 uptake for the regional variations in α_F is significant, as the error given mainly represents the error in the trend and in the global fossil fuel emissions. If we would have used the global average α_F of 1.4, the global oceanic CO_2 uptake would be estimated at 2.6 PgC/year.

For Mace Head the trend during the measurement period is -8.4 ± 0.7 per meg/year, significantly lower than the trend observed at Lutjewad. As we have discussed in Sect. 4.2, the existing gradients in CO_2 and O_2 between Lutjewad and Mace Head are increasing during the observation period. This is also reflected in the trend in APO. As the air flasks at Mace Head are sampled during restricted baseline conditions, the corrected OR (α_F = 1.45) as calculated by REMO, might not reflect the actual perceived OR of the measured samples, as REMO gives the perceived OR during all

ACPD
10, 13055–13090, 2010

circumstances. The global oceanic CO_2 uptake at Mace Head is therefore likely better estimated with the global average OR of 1.4. This leads to a global oceanic CO_2 uptake of 1.8 ± 0.8 PgC/year. As sampling conditions at Mace Head are less influenced by local or regional anthropogenic disturbance, the trend in APO at Mace Head is likely to give a better estimation of the global oceanic CO_2 uptake than the APO trend from Lutjewad. Correcting the estimation based on the Lutjewad APO trend for the regional perceived fossil fuel OR, does however bring the two estimated closer to each other, thereby correcting for the observed increasing gradients between both locations.

Our estimation of the global oceanic CO_2 uptake of 1.8 ± 0.8 PgC/year over the period 1998–2009 agrees within the error bars with e.g. Manning and Keeling (2006). They found a global oceanic CO_2 uptake of 1.9 ± 0.6 PgC/year over the period 1990–2000 and 2.2 ± 0.6 PgC/year over the period 1993–2003. Longer time series of observations at Mace Head should be able to identify whether our lower estimate is valid and whether it is an indication of a decreasing oceanic CO_2 sink.

5 Conclusions

In this paper we have presented the CO_2, $\delta O_2/N_2$ and APO data series of the flask sample measurements from Lutjewad atmospheric monitoring station in the Netherlands, Mace Head atmospheric research station in Ireland and the F3 platform in the Dutch part of the North Sea together with continuous measurements from F3. With this work and that of colleagues combined, the density of the (European) $\delta O_2/N_2$ observational network is increasing gradually. These observations can be used in model efforts (both forward and inverse) to provide additional insights into the carbon cycle, also in a quantitative sense.

The records from Lutjewad and Mace Head have been used to construct the gradient in CO_2 and O_2 between Lutjewad and Mace Head. The obtained gradient fits well with the gradients observed between Mace Head and other European stations. The observed change in the gradient between Lutjewad and Mace Head is 0.5 ppm over

ACPD
10, 13055–13090, 2010

the presented sampling period. We have also presented the $\delta O_2/N_2$ gradient between Lutjewad and Mace Head. The gradient between both locations is gradually increasing (i.e. becoming more negative) during the sampling period, the change is −20 per meg over the total period 2001–2008. The effect on O_2 is much stronger than on CO_2, which is reflected by the fact that APO shows an increased gradient between Lutjewad and Mace Head as well.

Correcting APO with a regionally perceived fossil fuel oxidative ratio leads to a more consistent estimation of the global oceanic CO_2 uptake. Our best estimate of the global oceanic CO_2 uptake is based on the Mace Head APO trend and is estimated at 1.8 ± 0.8 PgC/year. Longer data series will further improve the quality of the annual trends and the oceanic uptake. Using long-term observations of multiple locations in a region will further improve the APO trend estimation and thereby improve the accuracy of the marine CO_2 uptake estimate. It is therefore essential that model efforts focus on independently transporting CO_2 and O_2 (instead of APO) yielding model based OR estimates for longer time periods.

The collection of flask samples at Lutjewad, Mace Head and F3 will be continued in the future as well as the continuous measurements at F3. For the Lutjewad atmospheric monitoring station continuous CO_2 data is available since 2006 (van der Laan et al., 2009b). Combined continuous measurements of $\delta O_2/N_2$ and CO_2 will also be started at Lutjewad in the near future.

Acknowledgements. This research is supported by the European Integrated Projects CarboEurope and CarboOcean (contract numbers 505572 and 511176 (GOCE) respectively). The authors would like to thank F3, NAM, Shell and GdF Suez staff members for their support to this project. We are especially grateful for the generous ongoing logistic and technical support by GdF Suez. Furthermore the authors thank Centre for Isotope Research staff members B. A. M. Kers, J. K. Schut, H. G. Jansen, H. A. Been, A. T. Aerts-Bijma, J. J. Spriensma and J. C. Roeloffzen for their contributions.

ACPD
10, 13055–13090, 2010

References

Battle, M., Bender, M. L., Tans, P. P., White, J. W. C., Ellis, J. T., Conway, T., and Francey, R. J.: Global carbon sinks and their variability inferred from atmospheric O_2 and delta ^{13}C, Science, 287, 2467–2470, doi:10.1126/science.287.5462.2467, 2000.

Battle, M., Mikaloff Fletcher, S. E., Bender, M. L., Keeling, R. F., Manning, A. C., Gruber, N., Tans, P. P., Hendricks, M. B., Ho, D. T., Simonds, C., Mika, R., and Paplawsky, B.: Atmospheric potential oxygen: New observations and their implications for some atmospheric and oceanic models, Global Biogeochem. Cy., 20, GB1010, doi:10.1029/2005GB002534, 2006.

Bender, M. L., Ellis, T., Tans, P., Francey, R., and Lowe, D.: Variability in the O_2/N_2 ratio of southern hemisphere air, 1991–1994: Implications for the carbon cycle, Global Biogeochem. Cy., 10, 9–21, doi:10.1029/95GB03295, 1996.

Bender, M. L., Ho, D. T., Hendricks, M. B., Mika, R., Battle, M. O., Tans, P. P., Conway, T. J., Sturtevant, B., and Cassar, N.: Atmospheric O_2/N_2 changes, 1993–2002: Implications for the partitioning of fossil fuel CO2 sequestration, Global Biogeochem. Cy., 19, GB4017, doi:10.1029/2004GB002410, 2005.

Bender, M. L., Tans, P. P., Ellis, J. T., Orchardo, J., and Habfast, K.: A High-Precision Isotope Ratio Mass-Spectrometry Method for Measuring the O_2/N_2 Ratio of Air, Geochim. Cosmochim. Ac., 58, 4751–4758, doi:10.1016/0016-7037(94)90205-4, 1994.

Boden, T., Marland, G., and Andres, R. J.: Global CO_2 Emissions from Fossil-Fuel Burning, Cement Manufacture, and Gas Flaring: 1751–2006., Carbon Dioxide Information Analysis Center, Oak Ridge National Laboratory, Oak Ridge, Tennessee 37831–6335, 2009.

Bousquet, P., Gaudry, A., Ciais, P., Kazan, V., Monfray, P., Simmonds, P. G., Jennings, S. G., and O'Connor, T. C.: Atmospheric CO_2 concentration variations recorded at Mace Head, Ireland, from 1992 to 1994, Phys. Chem. Earth, 21, 477-481, doi:10.1016/S0079-1946(97)81145-7, 1996.

Chevillard, A., Karstens, U., Ciais, P., Lafont, S., and Heimann, M.: Simulation of atmospheric CO_2 over Europe and western Siberia using the regional scale model REMO, Tellus B, 54, 872–894, doi:10.1034/j.1600-0889.2002.01340.x, 2002.

Corbière, A., Metzl, N., Reverdin, G., Brunet, C., and Takahashi, A.: Interannual and decadal variability of the oceanic carbon sink in the North Atlantic subpolar gyre, Tellus B, 59, 168–178, doi:10.1111/j.1600-0889.2006.00232.x, 2007.

ACPD
10, 13055–13090, 2010

Derwent, R. G., Ryall, D. B., Manning, A., Simmonds, P. G., O'Doherty, S., Biraud, S., Ciais, P., Ramonet, M., and Jennings, S. G.: Continuous observations of carbon dioxide at Mace Head, Ireland from 1995 to 1999 and its net European ecosystem exchange, Atmos. Environ., 36, 2799–2807, doi:10.1016/S1352-2310(02)00203-0, 2002.

GLOBALVIEW-CO_2: Cooperative Atmospheric Data Integration Project – Carbon Dioxide. CD-ROM, NOAA ESRL, Boulder, Colorado, 2008.

IPCC: Climate Change 2007: The Physical Science Basis. Contribution of Working Group I to the Fourth Assessment Report of the Intergovernmental Panel on Climate Change, Cambridge University Press, Cambridge, United Kingdom and New York, NY, USA, 996 pp., 2007.

Jennings, S. G., McGovern, F. M., and Cooke, W. F.: Carbon Mass Concentration Measurements at Mace Head, on the West-Coast of Ireland, Atmos. Environ. A-Gen., 27, 1229–1239, doi:10.1016/S1352-2310(02)00203-0, 1993.

Keeling, R. F.: Development of an Interferometric Oxygen Analyzer for Precise Measurement of the Atmospheric O_2 Mole Fraction, PhD Thesis, Division of Applied Sciences, Harvard University, Cambridge, Massachusetts, 178 pp., 1988a.

Keeling, R. F.: Measuring Correlations between Atmospheric Oxygen and Carbon-Dioxide Mole Fractions – a Preliminary-Study in Urban Air, J. Atmos. Chem., 7, 153–176, doi:10.1007/BF00048044, 1988b.

Keeling, R. F., and Garcia, H. E.: The change in oceanic O_2 inventory associated with recent global warming, P. Natl. Acad. Sci. USA, 99, 7848–7853, doi:10.1073/pnas.122154899, 2002.

Keeling, R. F., Najjar, R. P., Bender, M. L., and Tans, P. P.: What Atmospheric Oxygen Measurements Can Tell Us About the Global Carbon-Cycle, Global Biogeochem. Cy., 7, 37–67, doi:10.1029/92GB02733, 1993.

Keeling, R. F. and Shertz, S. R.: Seasonal and Interannual Variations in Atmospheric Oxygen and Implications for the Global Carbon-Cycle, Nature, 358, 723–727, doi:10.1038/358723a0, 1992.

Kozlova, E. A., Manning, A. C., Kisilyakhov, Y., Seifert, T., and Heimann, M.: Seasonal, synoptic, and diurnal-scale variability of biogeochemical trace gases and O_2 from a 300-m tall tower in central Siberia, Global Biogeochem. Cy., 22, GB4020, doi:10.1029/2008GB003209, 2008.

ACPD

10, 13055–13090, 2010

Langenfelds, R. L., Francey, R. J., Steele, L. P., Battle, M., Keeling, R. F., and Budd, W. F.: Partitioning of the global fossil CO_2 sink using a 19-year trend in atmospheric O_2, Geophys. Res. Lett., 26, 1897–1900, doi:10.1029/1999GL900446, 1999.

Langmann, B.: Numerical modelling of regional scale transport and photochemistry directly together with meteorological processes, Atmos. Environ., 34, 3585–3598, doi:10.1016/S1352-2310(00)00114-X, 2000.

Machta, L. and Hughes, E.: Atmospheric Oxygen in 1967 to 1970, Science, 168, 1582–1584, doi:10.1126/science.168.3939.1582, 1970.

Manning, A. C. and Keeling, R. F.: Global oceanic and land biotic carbon sinks from the Scripps atmospheric oxygen flask sampling network, Tellus B, 58, 95–116, doi:10.1111/j.1600-0889.2006.00175.x, 2006.

Manning, A. C., Keeling, R. F., and Severinghaus, J. P.: Precise atmospheric oxygen measurements with a paramagnetic oxygen analyzer, Global Biogeochem. Cy., 13, 1107–1115, doi:10.1029/1999GB900054, 1999.

Neubert, R. E. M., Spijkervet, L. L., Schut, J. K., Been, H. A., and Meijer, H. A. J.: A computer-controlled continuous air drying and flask sampling system, J. Atmos. Ocean. Tech., 21, 651–659, doi:10.1175/1520-0426(2004)021, 2004.

Olivier, J. G. J. and Berdowski, J. J. M.: Global emissions sources and sinks, in: The Climate System, edited by: Berdowski, J., Guicherit, R., and Heij, B. J., A. A. Balkema Publishers/Swets & Zeitlinger Publishers, Lisse, The Netherlands, pp. 33–78., 2001.

Patecki, M. and Manning, A. C.: First results from shipboard atmospheric O_2 and CO_2 measurements over the North Atlantic Ocean, OCEANS 2007 – Europe, 1–6, doi:10.1109/OCEANSE.2007.4302351, 2007.

Popa, M. E., Gloor, M., Manning, A. C., Jordan, A., Schultz, U., Haensel, F., Seifert, T., and Heimann, M.: Measurements of greenhouse gases and related tracers at Bialystok tall tower station in Poland, Atmos. Meas. Tech. Discuss., 2, 2587–2637, 2009, http://www.atmos-meas-tech-discuss.net/2/2587/2009/.

Ramonet, M., Ciais, P., Aalto, T., Aulagnier, C., Chevallier, F., Cipriano, D., Conway, T. J., Haszpra, L., Kazan, V., Meinhardt, F., Paris, J.-D., Schmidt, M., Simmonds, P., Xueref-Remy, I., and Necki, J. N.: A recent build-up of atmospheric CO_2 over Europe. Part 1: observed signals and possible explanations, Tellus B, 62, 1–13, doi:10.1111/j.1600-0889.2009.00442.x, 2010.

Rödenbeck, C., Le Quere, C., Heimann, M., and Keeling, R. F.: Interannual variability in oceanic

ACPD

10, 13055–13090, 2010

biogeochemical processes inferred by inversion of atmospheric O-2/N-2 and CO_2 data, Tellus B, 60, 685–705, doi:10.1111/j.1600-0889.2008.00375.x, 2008.
Schuster, U. and Watson, A. J.: A variable and decreasing sink for atmospheric CO_2 in the North Atlantic, J. Geophys. Res.-Oceans, 112, C11006, doi:10.1029/2006jc003941, 2007.
Severinghaus, J. P.: Studies of the terrestrial O_2 and carbon cycles in sand dune gases and in Biosphere 2, PhD Thesis, Columbia University, New York, 1995.
Sirignano, C., Neubert, R. E. M., Rödenbeck, C., and Meijer, H. A. J.: Atmospheric oxygen and carbon dioxide observations from two European coastal stations 2000-2005: continental influence, trend changes and APO climatology, Atmos. Chem. Phys., 10, 1599–1615, doi:10.5194/acp-10-1599-2010, 2010.
Steinbach, J., Gerbig, C., Rödenbeck, C., Karstens, U., Thompson, R. L., Minejima, C., and Mukai, H.: The CO_2 release and Oxygen uptake from Fossil Fuel Emission Estimate (COFFEE) dataset: Effects from varying oxidative ratios, in prep., 2010.
Stephens, B. B.: Field-based Atmospheric Oxygen Measurements and the Ocean Carbon Cycle, PhD Thesis, Scripps Institution of Oceanography, University of California, San Diego, 222 pp., 1999.
Stephens, B. B., Bakwin, P. S., Tans, P. P., Teclaw, R. M., and Baumann, D. D.: Application of a differential fuel-cell analyzer for measuring atmospheric oxygen variations, J. Atmos. Ocean. Tech., 24, 82–94, doi:10.1175/JTECH1959.1, 2007.
Stephens, B. B., Keeling, R. F., Heimann, M., Six, K. D., Murnane, R., and Caldeira, K.: Testing global ocean carbon cycle models using measurements of atmospheric O_2 and CO_2 concentration, Global Biogeochem. Cy., 12, 213–230, doi:10.1029/97GB03500, 1998.
Stephens, B. B., Keeling, R. F., and Paplawsky, W. J.: Shipboard measurements of atmospheric oxygen using a vacuum-ultraviolet absorption technique, Tellus B, 55, 857–878, doi:10.1046/j.1435-6935.2003.00075.x, 2003.
Sturm, P., Leuenberger, M., Sirignano, C., Neubert, R. E. M., Meijer, H. A. J., Langenfelds, R., Brand, W. A., and Tohjima, Y.: Permeation of atmospheric gases through polymer O-rings used in flasks for air sampling, J. Geophys. Res.-Atmos., 109, D04309, doi:10.1029/2003JD004073, 2004.
Thompson, R. L., Manning, A. C., Gloor, E., Schultz, U., Seifert, T., Hänsel, F., Jordan, A., and Heimann, M.: In-situ measurements of oxygen, carbon monoxide and greenhouse gases from Ochsenkopf tall tower in Germany, Atmos. Meas. Tech., 2, 573–591, 2009, http://www.atmos-meas-tech.net/2/573/2009/.

ACPD
10, 13055–13090, 2010

Thompson, R. L., Manning, A. C., Lowe, D. C., and Weatherburn, D. C.: A ship-based methodology for high precision atmospheric oxygen measurements and its application in the Southern Ocean region, Tellus B, 59, 643–653, doi:10.1111/j.1600-0889.2007.00292.x, 2007.

Tohjima, Y.: Method for measuring changes in the atmospheric O_2/N_2 ratio by a gas chromatograph equipped with a thermal conductivity detector, J. Geophys. Res.-Atmos., 105, 14575–14584, doi:10.1029/2000JD900057, 2000.

Tohjima, Y., Mukai, H., Nojiri, Y., Yamagishi, H., and Machida, T.: Atmospheric O_2/N_2 measurements at two Japanese sites: estimation of global oceanic and land biotic carbon sinks and analysis of the variations in atmospheric potential oxygen (APO), Tellus B, 60, 213–225, doi:10.1111/j.1600-0889.2007.00334.x, 2008.

Uglietti, C.: Understanding the Carbon Cycle through Atmospheric Carbon Dioxide and Oxygen Observations, PhD Thesis, Climate and Environmental Physics, Physics Institute, University of Bern, Bern, Switzerland, 159 pp., 2009.

van der Laan, S., Neubert, R. E. M., Karstens, U., van der Laan-Luijkx, I. T., and Meijer, H. A. J.: Fossil fuel based CO_2 emissions in the Netherlands based on ambient measurements and an improved ^{222}Radon flux method, submitted to Tellus B, 2009a.

van der Laan, S., Neubert, R. E. M., and Meijer, H. A. J.: A single gas chromatograph for accurate atmospheric mixing ratio measurements of CO_2, CH_4, N_2O, SF_6 and CO, Atmos. Meas. Tech., 2, 549–559, 2009b, http://www.atmos-meas-tech.net/2/549/2009/.

van der Laan, S., Neubert, R. E. M., and Meijer, H. A. J.: Methane and nitrous oxide emissions in The Netherlands: ambient measurements support the national inventories, Atmos. Chem. Phys., 9, 9369–9379, doi:10.5194/acp-9-9369-2009, 2009.

van der Laan-Luijkx, I. T., Neubert, R. E. M., van der Laan, S., and Meijer, H. A. J.: Continuous measurements of atmospheric oxygen and carbon dioxide on a North Sea gas platform, Atmos. Meas. Tech., 3, 113–125, 2010, http://www.atmos-meas-tech.net/3/113/2010/.

Watson, A. J., Schuster, U., Bakker, D. C. E., Bates, N. R., Corbiere, A., Gonzalez-Davila, M., Friedrich, T., Hauck, J., Heinze, C., Johannessen, T., Kortzinger, A., Metzl, N., Olafsson, J., Olsen, A., Oschlies, A., Padin, X. A., Pfeil, B., Santana-Casiano, J. M., Steinhoff, T., Telszewski, M., Rios, A. F., Wallace, D. W. R., and Wanninkhof, R.: Tracking the Variable North Atlantic Sink for Atmospheric CO_2, Science, 326, 1391–1393, doi:10.1126/science.1177394, 2009.

ACPD

10, 13055–13090, 2010

WMO: Report of the 14th WMO/IAEA Meeting of Experts on Carbon Dioxide Concentration and Related Tracers Measurement Techniques, Helsinki, Finland, 10-13 September 2007, World Meteorological Organization, Geneva, Switzerland, 2009.

Worthy, D. E. J., Platt, A., Kessler, R., Ernst, M., and Racki, S.: Measurement Procedures and Data Quality, Canadian Baseline Program; Summary of progress to 2002, Meteorological Service of Canada, 97–120, 2003.

ACPD

10, 13055–13090, 2010

Table 1. CO_2 and O_2 trend and seasonality based on the fit of the data sets from each measurement site: Lutjewad, Mace Head and F3. The used fit is a linear combination of a linear trend and a 3-harmonic seasonal component.

	Lutjewad	Mace Head	F3
Trend CO_2 (ppm/year)	1.97 ± 0.07	1.90 ± 0.04	2.11 ± 0.04
Trend $\delta O_2/N_2$ (per meg/year)	-21.0 ± 0.9	-18.5 ± 0.7	-27.1 ± 0.6
Trend APO (per meg/year)	-10.6 ± 0.7	-8.4 ± 0.7	-13.2 ± 0.5
Amplitude CO_2 (ppm)	12.0 ± 0.6	14.0 ± 0.3	15.2 ± 0.1
Amplitude $\delta O_2/N_2$ (per meg)	114 ± 8	142 ± 6	144 ± 2
Amplitude APO (per meg)	64 ± 6	74 ± 6	111 ± 2
Day of maximum CO_2	72 (13 Mar)	107 (17 Apr)	84 (25 Mar)
Day of minimum CO_2	229 (17 Aug)	242 (30 Aug)	240 (28 Aug)
Day of minimum $\delta O_2/N_2$	90 (31 Mar)	42 (12 Feb)	49 (19 Feb)
Day of maximum $\delta O_2/N_2$	252 (9 Sep)	243 (31 Aug)	263 (19 Sep)
Day of minimum APO	84 (25 Mar)	40 (10 Feb)	15 (16 Jan)
Day of maximum APO	255 (12 Sep)	243 (31 Aug)	171 (20 Jun)

ACPD
10, 13055–13090, 2010

Table 2. CO_2, $\delta O_2/N_2$ and APO trend and seasonality from Lutjewad and Mace Head flask samples and for F3 from a combination of flask samples and continuous observations in comparison to observations from other European measurement locations. The error bars for the trends and amplitudes presented in this work are given in Table 1.

Location	Trend (per year)			Amplitude			Measurement Period (Flasks or Continuous) Reference
	CO_2 (ppm)	O_2/N_2 (per meg)	APO	CO_2 (ppm)	O_2/N_2 (per meg)	APO	
Lutjewad 53°24′ N, 6°21′ E	1.97	−21.0	−10.6	12.0	114	64	2000–2009 (F) (this work)
Mace Head 53°20′ N, 9°54′ W	1.90	−18.5	−8.4	14.0	142	74	1998–2009 (F) (this work)
F3 54°51′ N, 4°44′ E	2.11	−27	−13	15.2	144	111	2006–2009 (C and F) (this work)
Ochsenkopf 50°02′ N, 11°48′ E	1.6	−16	−9.7	15.5	135	43	2006–2008 (C) (Thompson et al., 2009)
Bialystok 53°13′ N, 23°01′ E	2.0	−23	x	25	161	43	2005–2008 (C) (Popa et al., 2009)
Shetland Islands 60°17′ N, 1°17′ W	2.2	−19	−7.2	15.4	163	95	2004–2008 (F) (Kozlova et al., 2008)
ZOTTO 60°48′ N, 89°21′ E	2.0	x	x	26.6	134	51	2005–2007 (C) (Kozlova et al., 2008)
Puy de Dôme 45°46′ N, 2°58′ E	1.2	−17	x	16.1	118	45	2004–2008 (F) (Uglietti, 2009)
Jungfraujoch 46°33′ N, 7°59′ E	1.8	−13	−5 to −22	9.9	76	21	2006–2008 (F) (Uglietti, 2009)

ACPD
10, 13055–13090, 2010

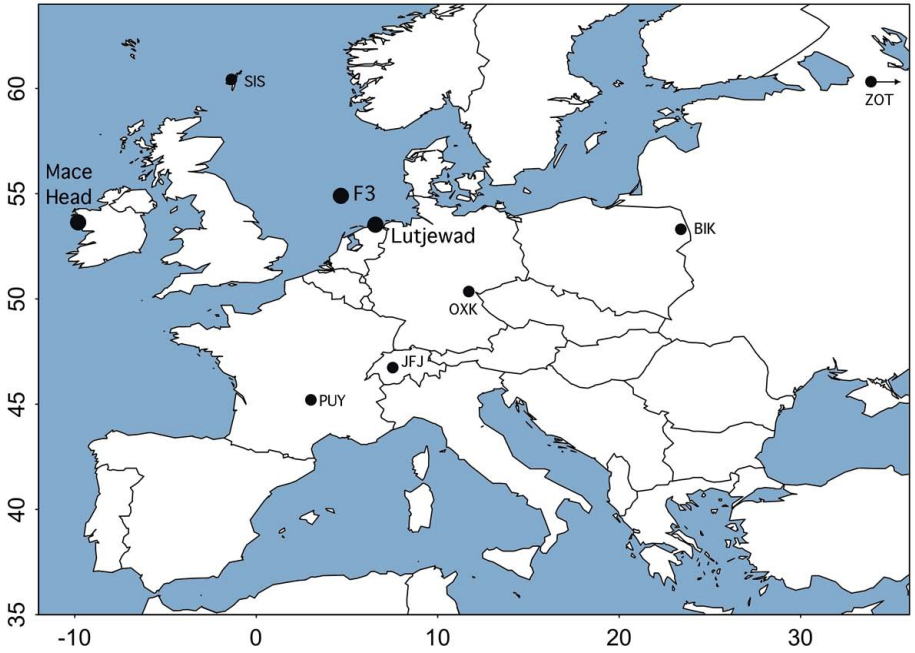

Fig. 1. Location of the three stations from which the flasks have been sampled: Lutjewad, Mace Head and F3. Also shown are the locations of other European measurements which are used for comparison. These are: Ochsenkopf (OXK), Bialystok (BIK), Shetland Islands (SIS), Zotino (ZOT), Puy de Dôme (PUY) and Jungfraujoch (JFJ).

ACPD
10, 13055–13090, 2010

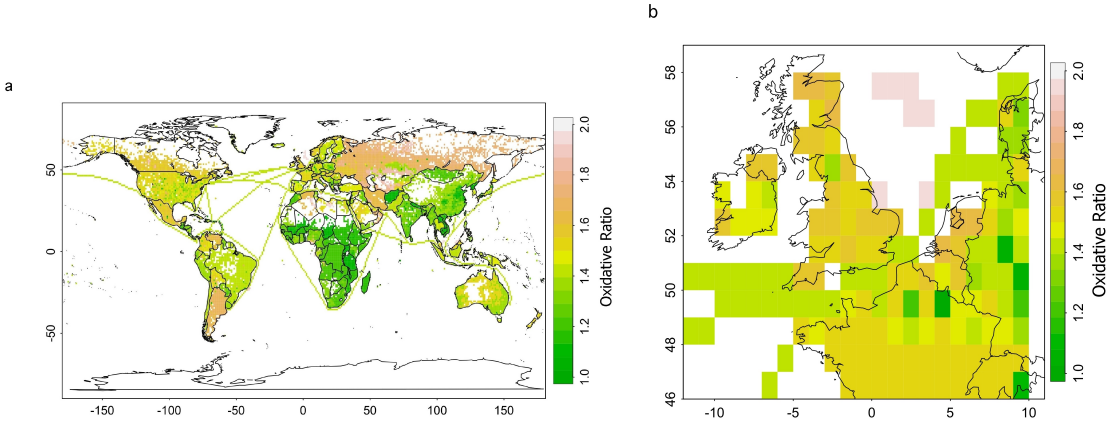

Fig. 2. The global distribution of the oxidative ratios from fossil fuel combustion **(a)** and the regional distribution at our sampling locations is shown in more detail **(b)** (Steinbach et al., 2010). White grid cells indicate that no data is available in the EDGAR database. For Lutjewad the grid cell just below the actual position of Lutjewad has therefore been used in this paper.

ACPD
10, 13055–13090, 2010

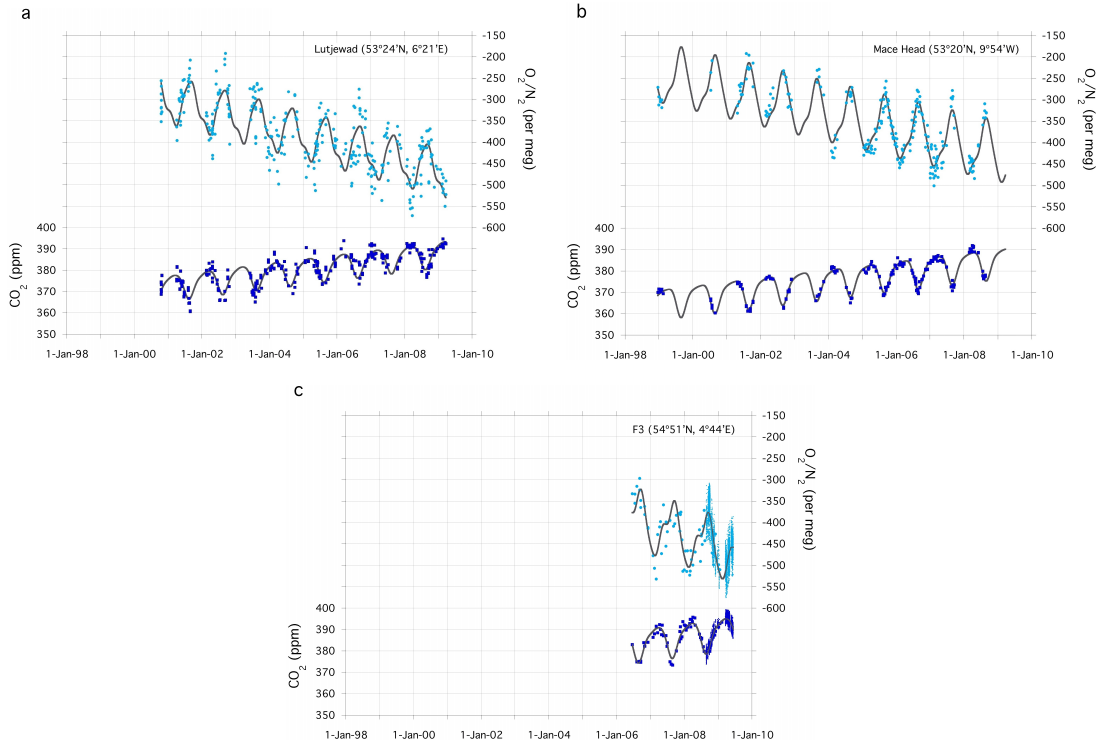

Fig. 3. Observations of the atmospheric O_2 (lighter circles) and CO_2 (darker squares) concentrations at station Lutjewad **(a)**, Mace Head **(b)** and F3 **(c)** during 2000–2009, based on flask measurements. The fits through the data points are a combination of a three harmonic function and a linear trend.

ACPD
10, 13055–13090, 2010

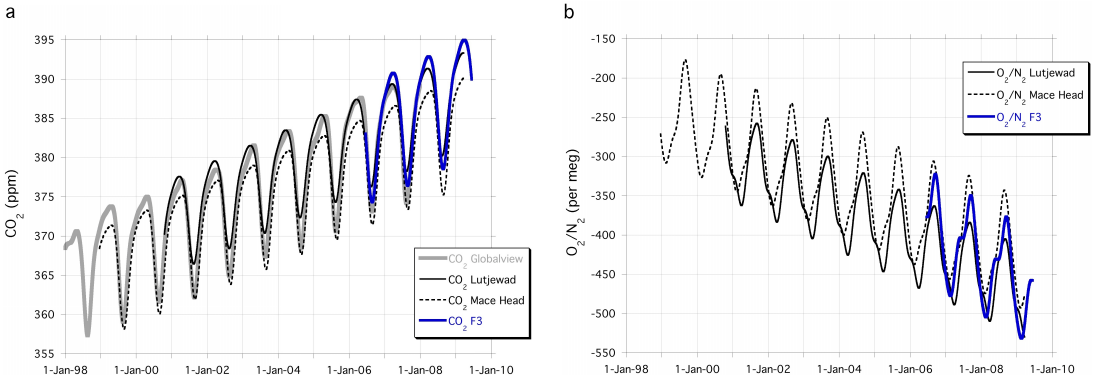

Fig. 4. Trend fits of CO_2 **(a)** and O_2 **(b)** at Lutjewad (solid black line), Mace Head (dashed black line) and F3 (solid blue line) during 2000–2009, based on flask measurements (and continuous measurements for F3). The fits are a linear combination of a three harmonic function and a linear trend through the data points (in Fig. 3). The CO_2 trends of the three measurement locations are shown in comparison to the CO_2 background reference concentration according to GLOBALVIEW-CO_2 (2008) (solid grey line) at latitude 53° N. The increasing gradients between Mace Head and Lutjewad are visible for both CO_2 and $\delta O_2/N_2$.

ACPD
10, 13055–13090, 2010

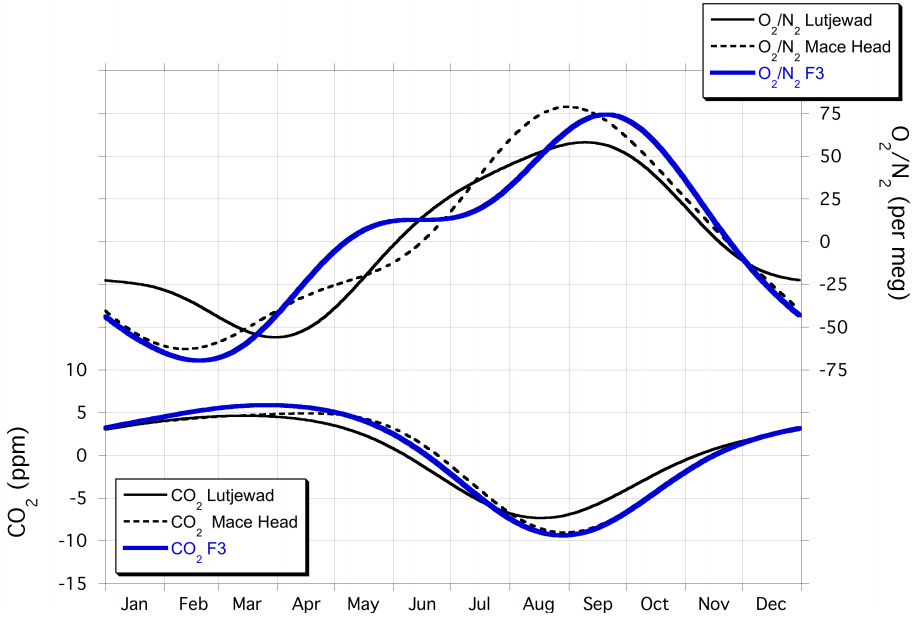

Fig. 5. The de-trended seasonal patterns of CO_2 and O_2 at station Lutjewad (black solid line), Mace Head (black dashed line) and F3 (blue solid line) during 2000–2009, based on flask measurements (and continuous measurements for F3).

ACPD
10, 13055–13090, 2010

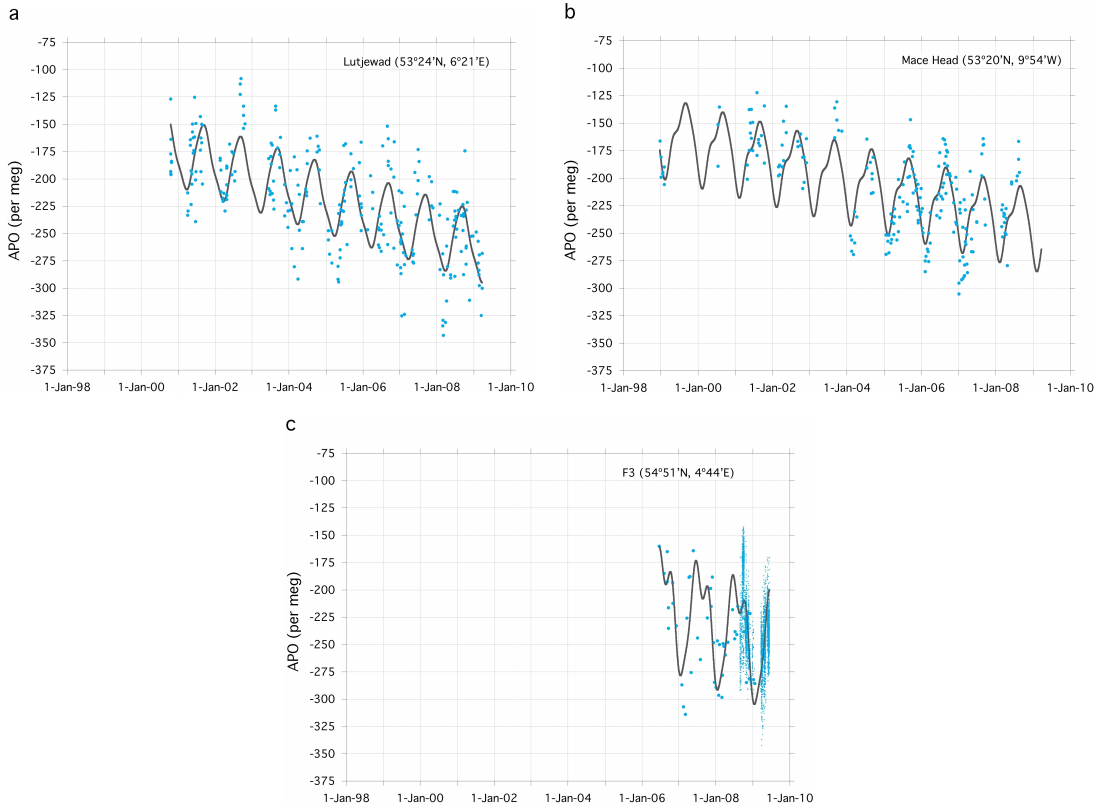

Fig. 6. Observations of the Atmospheric Potential Oxygen (APO) at station Lutjewad **(a)**, Mace Head **(b)** and F3 **(c)** during 2000–2009, based on flask measurements. The fits through the data points are a combination of a three harmonic function and a linear trend.

ACPD
10, 13055–13090, 2010

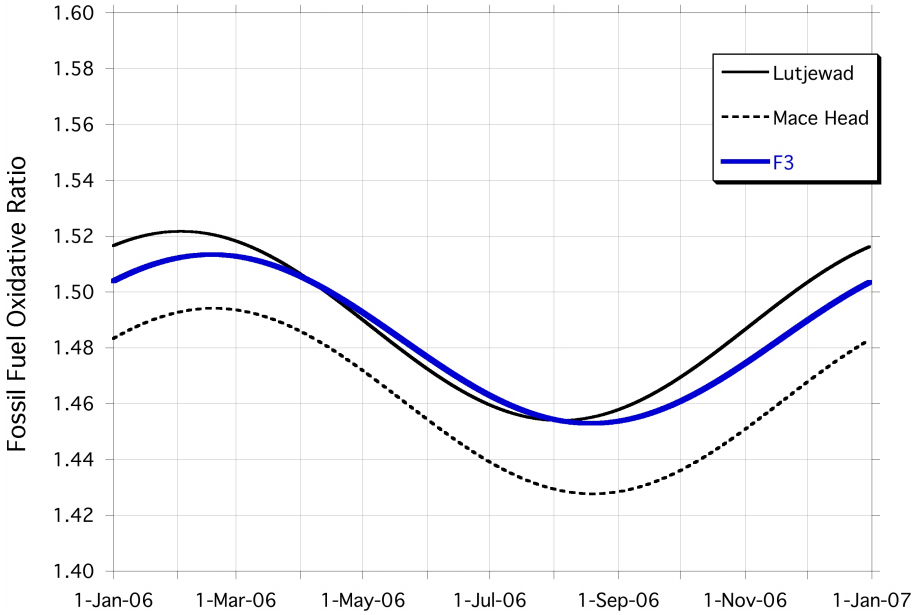

Fig. 7. Fit of the modelled data of fossil fuel CO_2 and O_2 for 2006 expressed as the fossil fuel oxidative ratio (OR) for our three measurement locations using REMO. The fit shows the seasonal variability in the average OR for each location during the course of the year as well as the spatial variability between the three sites. The OR at all sites differs significantly from the global mean OR of 1.4 as well as from its local emission based OR (EDGAR) as shown in Fig. 2a.

ACPD
10, 13055–13090, 2010